The Astrophysical Journal Letters, 884:L57 (5pp), 2019 October 20 https://doi.org/10.3847/2041-8213/ab4a82

Reynolds Number and Intermittency in the Expanding Solar Wind: Predictions Based on *Voyager* Observations

T. N. Parashar, M. Cuesta, and W. H. Matthaeus
Bartol Research Institute, Department of Physics and Astronomy, University of Delaware, Newark, DE, USA
Received 2019 September 9; accepted 2019 October 1; published 2019 October 21

Abstract

The large-scale features of the solar wind are examined in order to predict small-scale features of turbulence in unexplored regions of the heliosphere. The strategy is to examine how system size, or effective Reynolds number Re, varies, and then how this quantity influences observable statistical properties, including intermittency properties of solar wind turbulence. The expectation based on similar hydrodynamics scalings is that the kurtosis, of the small-scale magnetic field increments, will increase with increasing Re. Simple theoretical arguments as well as *Voyager* observations indicate that effective interplanetary turbulence Re decreases with increasing heliocentric distance. The decrease of scale-dependent magnetic increment kurtosis with increasing heliocentric distance is verified using a newly refined *Voyager* magnetic field data set. We argue that these scalings continue to much smaller heliocentric distances approaching the Alfvén critical region, motivating a prediction that the *Parker Solar Probe* spacecraft will observe increased magnetic field intermittency, stronger current sheets, and more localized dissipation, as its perihelion approaches the critical regions. Similar arguments should be applicable to turbulence in other expanding astrophysical plasmas.

Unified Astronomy Thesaurus concepts: Interplanetary turbulence (830); Heliosphere (711); Space plasmas (1544); Solar wind (1534); Plasma astrophysics (1261)

1. Introduction

Theories of turbulence, in particular Kolmogorov theory (Kolmogorov 1941a, 1941b, 1962; Frisch 1996) and its many variations, are frequently applied to understanding spacecraft observations in the interplanetary plasma (Horbury et al. 2008; Bruno & Carbone 2013; Chen 2016). In most instances these theories are invoked, either explicitly or implicitly, in a form appropriate to the regime of *universality* conjectured to apply in the limit of infinite Re (Kolmogorov 1941a, 1941b, 1962). However, it is well known based on experimental data, especially in hydrodynamics (Pope 2000), that the dimensionless Re, at attainable finite values, controls scaling of numerous statistical quantities, including the approach to an asymptotic dissipation rate and the scaling of higher-order moments or increments. There is substantial evidence mainly based on simulations that magnetohydrodynamics (MHD) and other plasma models exhibit analogous systematic variations with Reynolds-like numbers (Linkmann et al. 2015; Bandyopadhyay et al. 2018). The above studies were focused on the scaling of dissipation with Reynolds number. Here we are interested in a related but distinct quantity, the kurtosis of magnetic field at very small increments. Although it has been shown that the dissipation saturates with Re, it is not clear if kurtosis also saturates. For the hydrodynamic case, see Van Atta & Antonia (1980). No such study exists for plasmas at large Re as far as we are aware. Here we examine turbulence in the solar wind, quantifying variation of a specific intermittency parameter, the kurtosis of magnetic field increments, as the effective Re is varied. This is made possible by the wide range of effective Re encountered by *Voyager* as we show below.

In particular we are interested in the following question: how can scaling of *Voyager* observations of interplanetary turbulence with Re inform predictions about plasma turbulence in a broader context? The answer to this question is important not only to anticipate what will be observed by spacecraft such as *Parker Solar Probe* as well as *Solar Orbiter*, but also for observation of expanding plasmas in diverse astrophysical situations. We explore this possibility here, with specific predictions for *Parker Solar Probe* (Fox et al. 2016), by employing *Voyager* magnetic field observations (Matthaeus & Goldstein 1982; Ness & Burlaga 2001). The data allow examination of the behavior of effective turbulence Reynolds number and its possible effect on magnetic field fluctuations over a wide range of heliocentric distances. In a novel examination of this putative connection, we find that the Re decreases, and the kurtosis at a fixed physical scale decreases with increasing distance, with associated expectations concerning the roughness of the magnetic field. Extrapolating the observed scaling to lower heliocentric distances motivates the prediction that the spatial concentration of coherent structures increases approaching the Alfvén critical region from outside, an effect that *Parker Solar Probe* should soon measure. This Letter provides theoretical and observation details that motivate this prediction, and discusses further applications. In particular, the notion of Re needs to be considered with care, as kinetic plasmas such as the solar wind do not have a well-defined viscosity or resistivity that can be used to define Re. Instead one needs to consider an alternate interpretation of Re, related to the bandwidth available, for the cascade to proceed. We now discuss these definitions of Re.

2. Effective Reynolds Number

In hydrodynamics the value of kinematic viscosity ν enters into the definition of (large-scale) Reynolds number $\mathrm{Re} = uL/\nu$, for turbulence speed u, and energy containing (outer) scale L. For the weakly collisional plasma found in the solar wind, ν is meaningless, and an extension of the notion of Re requires a focus on its intended physical implications (Matthaeus et al. 2008). In (magneto)hydrodynamics the Reynolds number encompasses two related but distinct elements: dissipation (in

the form of ν or η), and the bandwidth available for turbulence to populate various scales. The first one is the notion of the relative importance of dissipative and convective processes. High Re at the outer scale L implies absence of dissipation, while at the Kolmogorov dissipation scale η the Re becomes unity. In fact, Re relates the outer (correlation) scale L and inner (Kolmogorov dissipation) scale η as $\mathrm{Re} = (L/\eta)^{4/3}$. In this second meaning, high Re implies a large bandwidth, perhaps many decades of scale, over which the cascade proceeds. The latter definition is more relevant for kinetic plasmas, e.g., the solar wind, where the notion of ν or η can not be defined. However, an inner scale, marking the end of the inertial range, is well defined and is typically $\sim d_i$.

Of course in hydrodynamics, large turbulence amplitudes at scale L act to push the Kolmogorov scale η to smaller values. This connection between the first and second meaning of Re will not be available for weakly collisional plasmas. However, the effective Reynolds number as a measure of the available bandwidth is of central relevance to the emergence of intermittency, as the production of phase coherence and structures depends on progressive effects of the cascade acting over a wide range of scales (Frisch et al. 1983; Wan et al. 2009). This is the underlying reason that kurtosis is expected to increase with Reynolds number (Sreenivasan & Antonia 1997). Hence, for a weakly collisional plasma, the Kolmogorov dissipation scale η may be reasonably replaced by the ion inertial scale d_i (or the thermal gyroradius if plasma beta becomes large), given that the observed inertial range at MHD scales terminates at the largest proton kinetic scale encountered by the direct energy cascade (Leamon et al. 1998; Chen et al. 2014). Accordingly, we adopt a definition of effective Reynolds number in terms of the system size L/d_i, or size of the inertial range, as $\mathrm{Re} = (L/d_i)^{4/3}$. In this study we intend to investigate whether this definition of Re has implications for plasma intermittency that are analogous to what is observed in hydrodynamic turbulence (Pope 2000). This connection has not been previously examined as far as we are aware.

Below we will employ this definition of effective Re and examine its behavior between 1 and 10 au in *Voyager* magnetic field data. The observational finding, backed by an elementary theoretical assessment, is that Re decreases with increasing heliocentric distance in the solar wind. Thus, even as the wind expands to fill the available volume, and in this sense becomes larger, the "system size" from the perspective of turbulence is decreasing.

Based on the determination of the radial behavior of Re, the next step will be an assessment of the behavior of a normalized fourth-order moment of the magnetic fluctuations, and its scaling with the Reynolds number. Kurtosis, the normalized fourth moment, measures the roughness of the magnetic field and appearance of coherent structures. The kurtosis of increments of a magnetic field Cartesian component time series $b(t)$ with time lag τ is defined as $\kappa(\tau) = \langle \Delta b(\tau)^4 \rangle / \langle \Delta b(\tau)^2 \rangle^2$ where $\Delta b(\tau) = b(t+\tau) - b(t)$ is the increment at a scale τ. Following typical practice in solar wind studies, we will exploit the highly supersonic and super-Alfvénic flow at speed V_{sw} to interpret statistical properties at time lags τ with spatial lags $r = -V_{\mathrm{sw}}\tau$, the so-called Taylor hypothesis. The use of Taylor's hypothesis has been shown to work well for first- and second-order statistics down to the ion inertial scale and smaller (Chhiber et al. 2018).

3. Theoretical and Observational Expectations

The expected variation of Re with heliocentric distance may be anticipated using simple arguments as follows: a von Karman–Howarth phenomenology has been shown to work well for explaining radial variations of turbulence and plasma properties of the solar wind, including correlation length and proton temperature (Zank et al. 1996; Breech et al. 2008). Temporarily ignoring expansion, a relevant pair of equations (Matthaeus et al. 1996) is $\frac{dZ^2}{dt} = -\frac{1}{2}\frac{Z^3}{L}$ and $\frac{dL}{dt} = Z$, where Z is turbulence amplitude and L the correlation scale. However, under a reasonable set of assumptions (Breech et al. 2008) the expansion effects drop out of the evolution equation for the correlation scale L. The solution behaves as $L(t) \sim \sqrt{t}$, which when employing the Taylor hypothesis becomes $L(R) \sim R^{1/2}$, where here R is heliocentric distance. Meanwhile, to a reasonable approximation the proton number density in the solar wind falls off as $n(R) \sim R^{-2}$, and by definition the proton inertial scale in the expanding solar wind behaves as $d_i(n) \sim n^{-1/2} \sim R$. Therefore, the Re may behave approximately as $\mathrm{Re} = (L/d_i)^{4/3} \sim (R^{1/2}/R)^{4/3} \sim R^{-2/3}$.

On the observational side, it is well established that the correlation scale varies with heliocentric distance (Klein et al. 1992; Zank et al. 1996). This variation is found (Ruiz et al. 2014) to be approximately $\sim R^{0.44}$ in a mixed latitude ensemble, although the results did not have a strong dependence on plasma beta.

Turning to the kurtosis at small spatial lags, we find very little in the MHD or plasma literature concerning expectations for its behavior as Re is varied. There are studies at fixed (or, uncontrolled) Re, of the scale-dependent kurtosis of primitive variables in simulations, and in solar wind and magnetosheath observations (Sorriso-Valvo et al. 1999; Macek et al. 2017; Chhiber et al. 2018). Some insight into scaling of kurtosis at kinetic scales has been obtained in relatively low Re kinetic simulations (Parashar et al. 2015). There are also studies of multifractal scalings, but again, as far as we are aware, always without regard for Re or its variation. In hydrodynamics the situation is more advanced both in experiments and in theory. The small-scale kurtosis of longitudinal increments should at zero separation approach the kurtosis of longitudinal spatial *derivatives*. A well-studied set of hydrodynamic experiments examined the dependence of these velocity derivative kurtoses on Re (Van Atta & Antonia 1980). The best fits of these data to the variation of $\kappa \sim \mathrm{Re}^{\gamma}$ are $\gamma \approx 0.16$–0.2. This nicely brackets an analytical estimate, based on phenomenological estimates as well as extensions of Kolmogorov–Obukhov treatments based on log-normal distributions of increments (Oboukhov 1962). These theoretical estimates are discussed in the same reference (Van Atta & Antonia 1980) and lead to, for example, $\gamma = 3\mu/4 = 3/16$ when the log-normal intermittency parameter μ takes the value 0.25. Here we intend to leverage on the variability of solar wind conditions in the *Voyager* data set to study such dependences on Re in kinetic plasmas such as the solar wind. The abovementioned hydrodynamic expectations anticipate the similar behavior we find below for solar wind turbulence.

4. *Voyager* Data and Analysis

The *Voyager* magnetic field data sets are an excellent choice for the present study due the wide range of distances, conditions, and parameters spanned. This extreme variation

allows for wide variations in Re and hence allows us to study the variation of average behavior of Re in this system. Therefore, we use 1.92 s cadence magnetic field vector data from the *Voyager 1* spacecraft. For the present study, we use a refined data set, explained below, covering the range from 1 au up to ∼10 au.

The publicly available *Voyager* magnetic field data set, at the time of this writing, requires additional work to make it useful for a statistical study. We choose not to remove any transients, such as shocks and field reversals, as the turbulence parameter variation provided by these transients is desirable for our purpose. After the cleanup procedure we employed this improved subset of *Voyager 1*MAG data, which will be made available for other purposes.

One problem with the previously available data is due to the large data gaps associated with regular lack of telemetry. The first task we perform is to make the time series uniform by filling in the missing data points with not-a-numbers (NaNs). The final time series has ∼60 million data points.

The data available from the NASA–NSSDC also have many intervals containing "calibration rolls" as well as unexplained "noise" that need to be removed before any reliable turbulence statistics can be computed. We clean the data using a series of techniques. These include application of obvious cutoffs (−50nT, 50nT), a Hampel filter where the outliers are replaced with NaNs instead of a median value, and, finally, visual inspection of high kurtosis regions to identify and filter out remaining bad data. We describe the technique in detail in a longer paper (M. Cuesta et al. 2019, in preparation). The final clean time series has ∼23.27 million data points and ∼37.74 million NaNs representing missing data or discarded bad data.

After the cleaning procedure, we bin the data into 450 bins, each approximately of 0.02 au. A significant number of these bins have no physical data points, and some have very few physical data points. For statistical significance, we exclude bins with less than 10,000 physical data points from our analysis. The remaining useful data set comprises 328 bins, each having >10,000 points. For data quality purposes, we then compute the kurtosis at a small lag for the data in each bin. This helps further identify bins with potential bad data points as κ would be anomalously high for large unphysical discontinuities. Some retained bins contain what appears to be upstream waves (Smith et al. 1983) or similar plasma activity that cause κ to attain anomalously small values. We recall that using single-spacecraft data, we employ increments at very small time lags, and the Taylor hypothesis, to estimate radial magnetic field derivatives.

The two-time vector autocorrelation function of magnetic field is defined as

$$C_R(\tau) = \frac{\langle \boldsymbol{b}(t)\cdot\boldsymbol{b}(t+\tau)\rangle}{\langle |\boldsymbol{b}(t)|^2\rangle}, \quad (1)$$

where $\boldsymbol{b} = \boldsymbol{B} - \langle \boldsymbol{B}\rangle$. The outer scale is computed, using the Taylor frozen-in flow hypothesis, as the scale where the autocorrelation drops to $1/e$. In particular, we estimate the correlation scale as $L = V_{\rm sw}\tau_o$ where τ_o is the lag at which the two-time correlation of the magnetic field decreases to $1/e$. With these definitions, the effective Reynolds number can be computed as $Re = \left(\frac{L}{d_i}\right)^{4/3}$ where d_i is the ion inertial length c/ω_{pi} , chosen to represent the scale at which the inertial range terminates. The ion (proton) inertial length is computed in each bin by appropriate averages of the number density recorded by the *Voyager* plasma (PLS) plasma instrument. Note that choosing the electron inertial length as the inner scale would simply shift the Re by a constant value.

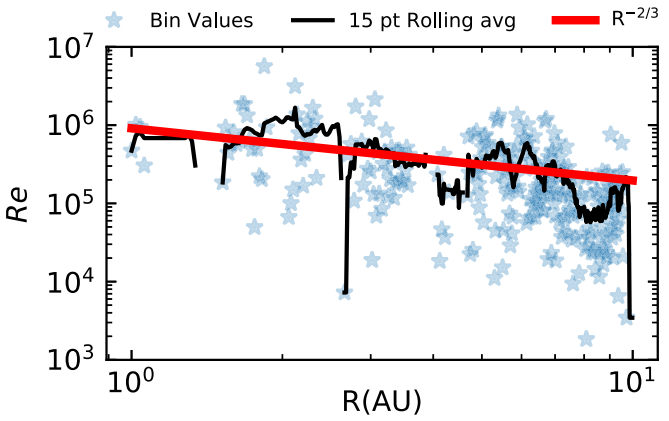

Figure 1. Effective Reynolds number as a function of heliocentric distance. Blue stars represent the value within a local bin. Black curve is a 15 point running average of these values. The red line indicates the anticipated decrease based on the elementary estimate presented in the text.

To approximate the kurtosis of magnetic field derivatives, we compute increments at the smallest possible physical scale covered by *Voyager*. To this effect, we choose $\Delta \sim 10d_i$, a small scale covered by the instrument resolution at 1 au and beyond. Interestingly, $10d_i$ is not too far from the expected Taylor scale in the solar wind (∼10–30d_i; Matthaeus et al. 2008).

5. Results

Figure 1 shows the effective Re computed from the magnetic field, as a function of heliocentric distance in the 1–10 au *Voyager* 1 data set. Blue stars represent the local value of Re in each of the 328 bins, each approximately 0.02 au wide in heliocentric distance. Significant variability is present in the Re, consistent with variable turbulence conditions (Tu & Marsch 1995), such as stream structure, coronal mass ejections, etc. There are some bins in which wave activity may modify the results. To get a better view of the average behavior of Re, we plot a 15 point running average of the blue stars. A clear trend for Re to drop with heliocentric distance can be seen. The elementary estimate of Re $\sim R^{-2/3}$, based on $L \sim \sqrt{R}$ and $d_i \sim R$, is overplotted as a thick red line. We emphasize the point that *this is not a fit of any kind*: the average Re follows a trend similar to the simple theoretical prediction. The turbulence "system size" or effective Re in the expanding solar wind in fact decreases with increasing radial distance.

According to the hydrodynamic analogy, a systematic decrease in Re should be reflected in a decrease in the kurtosis of increments computed at very small lags. This expectation would be obtained whenever the turbulence is fully developed, i.e., it is not too close to its injection or initiation. Having observed a systematic decrease in Re, we now examine the small-scale magnetic kurtosis in the same data set as a surrogate for the kurtosis of the longitudinal magnetic derivative. We compute the kurtosis at a lag of $10d_i$, where the distance is computed from time lag, using Taylor's hypothesis, using the average radial plasma velocity for the conversion.

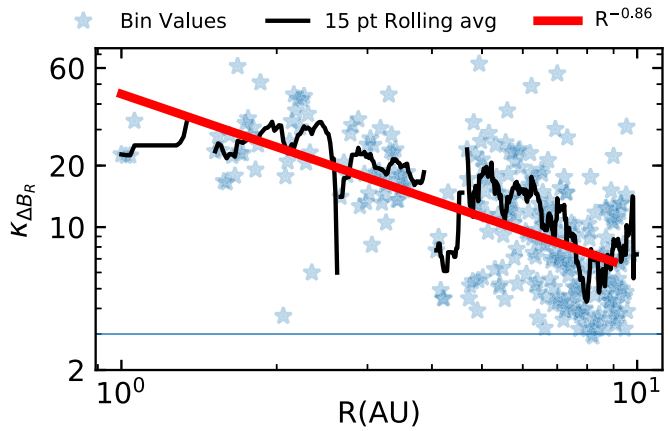

Figure 2. Kurtosis of ΔB_R at a lag of $10d_i$. Blue stars represent the value inside a local bin; black curve is a 15 point running average of these values. Horizontal blue line represents the kurtosis for Gaussian noise. Red line is a power-law fit to the points as there is yet no theory for how kurtosis should vary with Re in a plasma.

Figure 2 shows the kurtosis of the increment of the radial magnetic field component at the scale $10d_i$ as a function of heliocentric distance. Blue stars show value of kurtosis in each of the 328 bins, the black curve shows a 15 point running average, and the red line shows a power-law fit to the data with an approximate dependence $\kappa \sim R^{-0.86}$. As expected, the kurtosis drops for a larger heliocentric distance, along with the decrease of effective Reynolds number with increasing distance. Points that have lower kurtosis appear in the same regions where Re drops. However, these anomalously low points do not significantly affect the overall conclusion that both Re and κ decrease systematically with increasing heliocentric distance.

6. Conclusions

The above study, based on analysis of *Voyager* 1 magnetic field data, shows two main results that are established firmly by the observations. First, (I) the effective Reynolds number, as defined based on the extent of the inertial range, decreases systematically in the interplanetary medium between 1 and 10 au. Second (II) the kurtosis of magnetic component increments computed at the tail end of the inertial rage is also found to decrease with increasing heliocentric distances.

Potentially interesting physics comes in examining the relationship between these results. In fact, the reasoning that connects these two findings may be cast in more than one framework:

First, one might simply assume that the effective Re is fully equivalent to the ordinary Re, and then further assert that a relationship such as the hydrodynamic relation $\kappa \sim \mathrm{Re}^{\gamma} \sim \mathrm{Re}^{2\mu/4}$ also is obtained for a weakly collisional plasma. As we pointed out earlier, such a scaling can be obtained on purely empirical grounds. Or, it can be deduced from Refined Similarity (Kolmogorov 1962), augmented by Obukhov's scaling hypothesis (Oboukhov 1962) that parameterizes anomalous scaling of increments with L/η (which here becomes L/d_i by a separate argument). While this reasoning may appeal more strongly to formal turbulence theory, we recall that a Refined Similarity hypothesis has not been firmly established for a collisionless plasma (although there have been preliminary discussions of this; Merrifield et al. 2005; Chandran et al. 2015).

A second argument for the relationship of results I and II rests on understanding how the nonlinearities in turbulence, the most essential of which are *quadratic*, give rise dynamically to the formation of coherent structures. Nonlinear spectral transfer forms coherent structures, without direct involvement of dissipation, and progressively at a smaller scale (Frisch et al. 1983; Wan et al. 2009, 2012). This is evidenced, in both ideal and dissipative MHD, by the monotonic increase in *filtered* kurtosis (high pass filtered) at scale ℓ, as the bandpass scale decreases. Given that transfer is mainly local in scale (Verma et al. 2005), it follows that an inertial range with greater bandwidth will incorporate a greater number of octaves of transfer over which the coherent structures may form and intensify. Thus, larger systems, i.e., larger L/η or L/d_i, will have stronger coherent structures and higher small-scale kurtosis. But this implies immediately that $\kappa(10d_i)$ will decrease with effective Re as we have defined it. It is noteworthy that this second line of reasoning takes no explicit position on the relationship between coherent structures and dissipation, nor does it assume a refined similarity hypothesis, in contrast to the first line of reasoning. For this reason we prefer, at this time, the second track for connecting results I and II, although we do not doubt that the more formal relationships may be established more firmly in the future.

Having completed this excursion into the turbulence theoretic basis for relating I and II, we now may view the behavior of the kurtosis at $10d_i$ as a *consequence* of the decrease in effective Re at larger heliocentric radial distance. Such a connection has interesting implications beyond the magnetic field observed by *Voyager* in the outer heliosphere.

One major implication is the potential for extrapolating these results to other expanding astrophysical plasmas. We would expect, based on the arguments above, that other systems engaged in an approximate spherical expansion, with evolving von Karman turbulence, will also admit a baseline estimate of effective Re scaling as $\mathrm{Re}\sim\mathrm{R}^{-2/3}$. Turbulence properties that scale with Re will systematically respond to this scaling, enabling, in principle, a variety of predictions for expanding systems such as galactic winds, supernova remnants, etc. The decrease in kurtosis, or inverse filling factor, of coherent current structures is only one such prediction.

Closer to home, we are tempted to extrapolate the present results *inward*, toward the corona, but outside the Alfvén critical region. Such an extrapolation finds some partial support in correlation length scalings in radius from *Helios* and Ulysses (Ruiz et al. 2014) that behave as $L \sim R^{0.43}$ and density scalings (McComas et al. 2000) that remain close to $n \sim R^{-2}$ everywhere in the heliosphere on average. Encouraged by this, one may extrapolate that effective Re *increases* moving toward the inner interplanetary region where the magnetic control imposed by the corona gives way to the turbulent solar wind (DeForest et al. 2016). Approaching this region from outside, we expect that as Re increases, the kurtosis at small scales (multiples of d_i) will *increase*. This becomes, in effect a prediction for the recently launched *Parker Solar Probe* and the upcoming *Solar Orbiter* spacecraft: as these missions explore the heliosphere approaching the Alfvén critical region, we expect an increase in the frequency and intensity of magnetic discontinuities and current sheets. This should be indicted by higher-order statistics such as the kurtosis at small scales. There may be associated

implications such as stronger concentrations of dissipation and heating (Osman et al. 2012), a possibility we have not pursued here. There are reasons to believe that the turbulence is sustained well below the the Alfvén critical surface (Adhikari et al. 2019), but the nature of turbulence and its driving differs in that region (the corona). We do not attempt to extend our prediction beyond this point at present. As a step toward supporting the present prediction, we are currently processing *Helios* data to confirm this effect down to 0.3 au. *Helios* data have a time cadence much longer than the expected d_i, and hence the predictions for very small-scale increments can not be computed using *Helios*. Hence, these results will be limited to the middle of inertial range kurtoses. Our *Helios* results will be presented in a separate publication, as we anxiously await the relevant *Parker Solar Probe* analyses. We may anticipate that there will be further interesting consequences of the systematic variation of interplanetary effective Re that will be examined in future study.

The authors are thankful to Chuck Smith for useful discussions. This research is supported in part by the NASA Heliophysics Guest Investigator Program (80NSSC19K0284, NNX17AB79G) and Supporting Research (80NSSC18K1648) and by the ISOIS Parker Solar Probe Project though Princeton subcontract SUB0000165.

ORCID iDs

T. N. Parashar https://orcid.org/0000-0003-0602-8381
W. H. Matthaeus https://orcid.org/0000-0001-7224-6024

References

Adhikari, L., Zank, G. P., & Zhao, L.-L. 2019, ApJ, 876, 26
Bandyopadhyay, R., Oughton, S., Wan, M., et al. 2018, PhRvX, 8, 041052
Breech, B., Matthaeus, W. H., Minnie, J., et al. 2008, JGRA, 113, A08105
Bruno, R., & Carbone, V. 2013, LRSP, 10, 2
Chandran, B. D. G., Schekochihin, A. A., & Mallet, A. 2015, ApJ, 807, 39
Chen, C., Leung, L., Boldyrev, S., Maruca, B., & Bale, S. 2014, GeoRL, 41, 8081
Chen, C. H. K. 2016, JPlPh, 82, 535820602
Chhiber, R., Chasapis, A., Bandyopadhyay, R., et al. 2018, JGRA, 123, 9941
DeForest, C., Matthaeus, W., Viall, N., & Cranmer, S. 2016, ApJ, 828, 66
Fox, N., Velli, M., Bale, S., et al. 2016, SSRv, 204, 7
Frisch, U. 1996, Turbulence (Cambridge: Cambridge Univ. Press)
Frisch, U., Pouquet, A., Sulem, P.-L., & Meneguzzi, M. 1983, JMTAS, 1983, 191
Horbury, T. S., Forman, M., & Oughton, S. 2008, PhRvL, 101, 175005
Klein, L., Matthaeus, W., Roberts, D., & Goldstein, M. 1992, Solar Wind Seven (Amsterdam: Elsevier), 197
Kolmogorov, A. 1941a, DoSSR, 30, 301
Kolmogorov, A. N. 1941b, DoSSR, 32, 16
Kolmogorov, A. N. 1962, JFM, 13, 82
Leamon, R. J., Smith, C. W., Ness, N. F., Matthaeus, W. H., & Wong, H. K. 1998, JGRA, 103, 4775
Linkmann, M. F., Berera, A., McComb, W. D., & McKay, M. E. 2015, PhRvL, 114, 235001
Macek, W., Wawrzaszek, A., Kucharuk, B., & Sibeck, D. 2017, ApJL, 851, L42
Matthaeus, W., & Goldstein, M. 1982, JGR, 87, 6011
Matthaeus, W., Weygand, J., Chuychai, P., et al. 2008, ApJL, 678, L141
Matthaeus, W. H., Zank, G. P., & Oughton, S. 1996, JPlPh, 56, 659
McComas, D., Barraclough, B., Funsten, H., et al. 2000, JGRA, 105, 10419
Merrifield, J., Müller, W.-C., Chapman, S., & Dendy, R. 2005, PhPl, 12, 022301
Ness, N. F., & Burlaga, L. F. 2001, JGRA, 106, 15803
Oboukhov, A. 1962, JFM, 13, 77
Osman, K., Matthaeus, W., Wan, M., & Rappazzo, A. 2012, PhRvL, 108, 261102
Parashar, T. N., Matthaeus, W. H., Shay, M. A., & Wan, M. 2015, ApJ, 811, 112
Pope, S. B. 2000, Turbulent Flows (Cambridge: Cambridge Univ. Press)
Ruiz, M. E., Dasso, S., Matthaeus, W., & Weygand, J. 2014, SoPh, 289, 3917
Smith, C. W., Goldstein, M. L., & Matthaeus, W. H. 1983, JGRA, 88, 5581
Sorriso-Valvo, L., Carbone, V., Veltri, P., Consolini, G., & Bruno, R. 1999, GeoRL, 26, 1801
Sreenivasan, K. R., & Antonia, R. 1997, AnRFM, 29, 435
Tu, C., & Marsch, E. 1995, SSRv, 73, 1
Van Atta, C., & Antonia, R. 1980, PhFl, 23, 252
Verma, M. K., Ayyer, A., & Chandra, A. V. 2005, PhPl, 12, 082307
Wan, M., Matthaeus, W., Karimabadi, H., et al. 2012, PhRvL, 109, 195001
Wan, M., Oughton, S., Servidio, S., & Matthaeus, W. H. 2009, PhPl, 16, 080703
Zank, G., Matthaeus, W., & Smith, C. 1996, JGRA, 101, 17093